Electronic Supplementary Material (ESI) for Nanoscale.
This journal is © The Royal Society of Chemistry 2017

Supporting Information

Analytical, numerical, and experimental studies of viscoelastic effects on the performance of soft piezoelectric nanocomposites

Jing Li[1,2,5], *Zhiren Zhu*[3], *Lichen Fang*[1,2], *Shu Guo*[3], *Ugur Erturun*[4], *Zeyu Zhu*[1,2], *James E. West*[1,4], *Somnath Ghosh*[1,2,3], *Sung Hoon Kang*[1,2,*]

1. Department of Mechanical Engineering, Johns Hopkins University, Baltimore, MD 21218, USA.
2. Hopkins Extreme Materials Institute, Johns Hopkins University, Baltimore, MD 21218, USA.
3. Departments of Civil Engineering, Johns Hopkins University, Baltimore, MD 21218, USA.
4. Department of Electrical & Computer Engineering, Johns Hopkins University, Baltimore, MD 21218, USA.
5. Hubei Key Laboratory of Advanced Technology for Automotive Components, Wuhan University of Technology, Wuhan, Hubei 430070, PR China.

* Corresponding author: Sung Hoon Kang (shkang@jhu.edu)

Contents

1. Derivation of the piezoelectric constant (d_{33}) calculation under quasi-static loading conditions

(1) Derivation for equation (6)

As mentioned in the main text, a viscoelastic material loses energy when a load is applied, then removed. And, the area of hysteresis loop observed in the stress–strain curve is equal to the energy lost during the loading cycle. Therefore, viscously dissipated energy density (U_D) (the pink area in Figure 2) can be obtained by subtracting recovery energy (U_R) from deformation energy (U_S) as below:

$$U_D = U_S - U_R \qquad \text{(S1)}$$

and

$$U_S = \frac{1}{2} E_d {\varepsilon_s}^2 \qquad \text{(S2)}$$

$$U_R = \frac{1}{2} E_r {\varepsilon_r}^2 \qquad \text{(S3)}$$

where ε_s is the deformation strain ($\varepsilon_s = \sigma/E_d$), E_d is the loading deformation modulus, ε_r is the recovery strain ($\varepsilon_r = \sigma/E_r$), and E_r is the unloading recovery modulus.

Therefore, the energy density of viscous dissipation (U_D) (the pink area in Figure 2) can be obtained as

$$U_D = \frac{1}{2}\left(\frac{1}{E_d} - \frac{1}{E_r}\right)\sigma^2 \qquad \text{(S4)}$$

(2) Derivation for equation (7)

Under the quasi-static loading condition, the stored deformation energy density (U_S) and viscously dissipation energy density (U_D) of the composite material system can be obtained from the loading deformation/unloading recovery moduli, given as

$$U_S = \frac{1}{2} E_d {\varepsilon_s}^2 = \frac{1}{2}\frac{\sigma^2}{E_d} \qquad \text{(S5)}$$

$$U_D = \frac{1}{2}\left(\frac{1}{E_d} - \frac{1}{E_r}\right)\sigma^2 \qquad \text{(S6)}$$

Therefore, the effectively converted strain energy density (U_E) can be described as

$$U_E = U_S - U_D = \frac{\sigma^2}{2E_r} \quad \text{(S7)}$$

Due to the fact that the electric potential energy is generated from the applied mechanical energy (U_{piezo}) among the piezoelectric particles, mechanical energy should be transferred to piezoelectric particles for electrical outputs. Additionally, it is assumed that nanofillers is too small to affect the stress distribution throughout the p-NC and the strain energy is uniformly distributed. The effective converted strain energy (U_E) among the piezoelectric nanoparticles can be written as:

$$U_E = V_{piezo}U_E = V_{piezo}(U_S - U_D) = \frac{V_{piezo}\sigma^2}{2E_r} \quad \text{(S8)}$$

where V_{piezo} is the volume of piezoelectric particles.

Combining with the piezoelectric constant equation (4) in the main text ($\sigma_3 = \sigma$ in this case), the quasi-static piezoelectric constant in the polarization direction (d_{33}) of the p-NCs can be obtained as

$$d_{33} = \varepsilon_{p-NC}\sqrt{\frac{V_{piezo}}{VE_r\varepsilon_{piezo}}} \quad \text{(S9)}$$

where ε_{piezo} is the permittivity of the piezoelectric particle and ε_{p-NC} is the permittivity of the p-NC.

2. Fabrication processes and the scanning electron microscopy (SEM) images of piezoelectric nanocomposites

(1) The fabrication process of the piezo nanocomposite (p-NC) is described as follows (Figure S1).

STEP 1: Carbon nanotubes (CNTs) and $BaTiO_3$ nanoparticles (BTO NPs) were first dispersed in absolute ethyl alcohol (ACS reagent, ≥99.5%, available from Sigma Aldrich) by magnetic stirring for 5 hrs followed by ultrasonication for 60 min.

STEP 2: The BTO/CNTs/alcohol solution was subsequently mixed with the PDMS monomer (Sylgard 184 from Dow Chemical) using revolutionary mixer (KK-400W, Mazerustar) for 270 seconds. The mixture was placed in a vacuumed oven at 70°C until the alcohol was completely evaporated.

STEP 3: The PDMS curing agent was added to the mixture, which was then uniformly dispersed using revolutionary mixer (KK-400W, Mazerustar) for 180 seconds. The mass ratio between the PDMS monomer and curing agent was adjusted to control the mechanical properties. Then, the uncured BTO/CNTs/PDMS mixture was poured to a mold and degassed in a vacuum chamber.

STEP 4: The mixture was then cured in an oven (Lindberg Blue M from Thermo Fisher Scientific) at 120 °C for 20 minutes. Subsequently, the solidified p-NC was put at room temperature for 24 hours to ensure that the p-NC was completely cured. The synthesized p-NC could be cut into any shape and size according to experimental requirements.

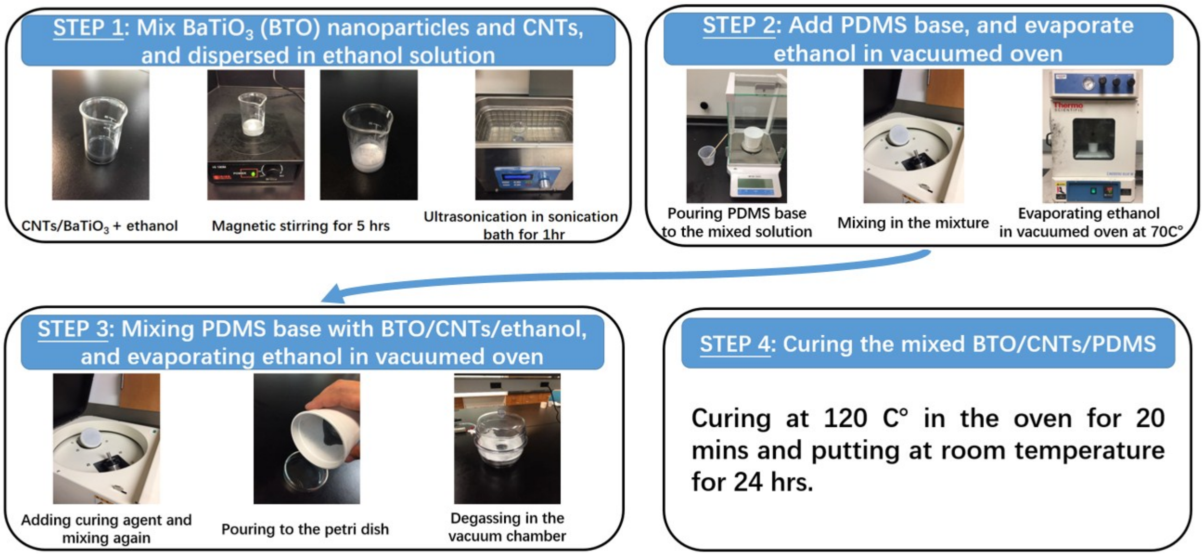

Figure S1. Schematic diagrams of the piezocomposite synthesis process.

(2) A schematic diagram of the p-NC with Au/Cr electrodes and a scanning electron microscopy (SEM) image of the surface of an electrode and cross section of the p-NC.

The Au/Cr metal was deposited to the top and bottom side of the p-NC as the conductive electrode by using sputtering (See Figure S2 (a) for a schematic). The thickness of the Au/Cr electrode was around 200 nm. Figure S2 (b) is the SEM image of the surface of the p-NC with Au/Cr electrode. Although there are “nano-island” and grain boundaries on the surface, the tested conductivity (> 3×10^{7} S/m) of the Au/Cr electrode is good. Figure S2 (c) shows the cross-sectional scanning electron microscopy (SEM) images of a p-NC. The inset in Figure S2 (c) is the magnified SEM image of the agglomerated $BaTiO_3$ nanoparticles distributed in the PDMS matrix.

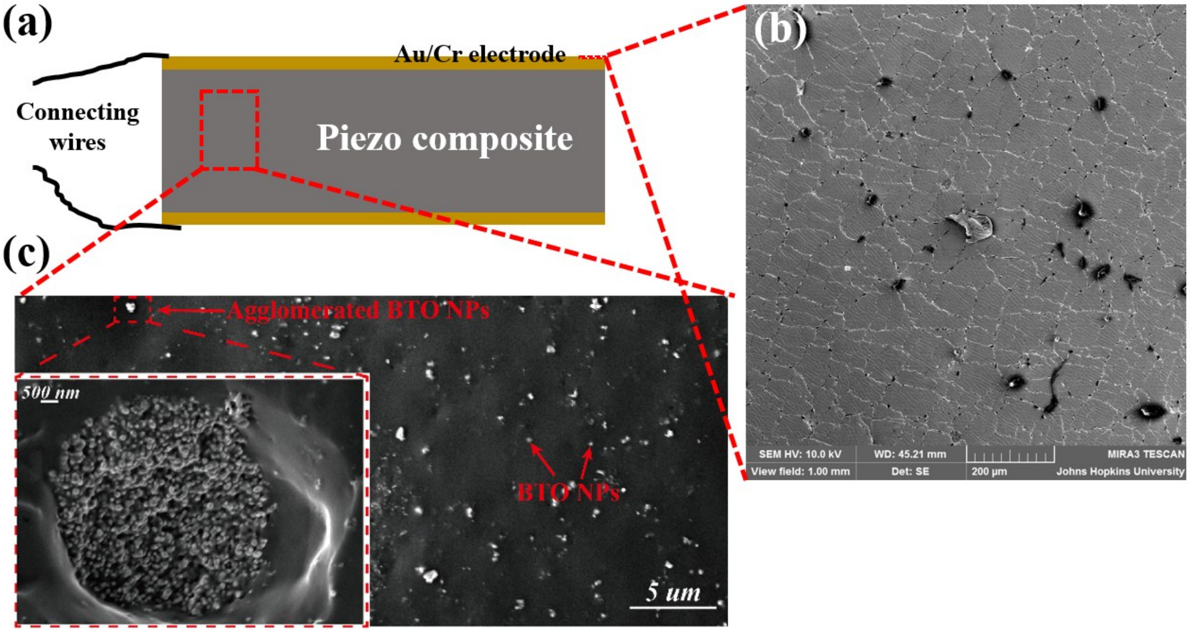

Figure S2. (a) Schematic diagram of the p-NC with Au/Cr electrodes and connecting wires. The connecting was bonded to the electrode surface using sliver paste. (b) SEM image of the surface of the p-NC with Au/Cr electrode. (c) A cross-sectional SEM image of a p-NC. The white particles are the $BaTiO_3$ nanoparticles, while the inset is the magnified SEM image of the agglomerated $BaTiO_3$ nanoparticles.

3. Stress-strain curves of the p-NCs and pure PMDS with different matrix mixing ratios

The stress-strain curves of p-NC and pure PDMS with different matrix mixing weight ratios were measured by MTS Insight 5 electromechanical test system as shown in Figure S3. The mixing ratios (λ) between PDMS monomer and curing agent were 5:1, 10:1 and 20:1, respectively. The results demonstrate that changing the mixing ratio of PDMS monomer and curing agent will lead to different mechanical properties of the pure PDMS polymer. Then, the varying mechanical behaviors of the PDMS matrix will have the same influence on the p-NCs. For example, when the p-NC mixtures were cured at 120 °C, the tensile moduli of 5:1, 10:1 and 20:1 p-NC were 1.32 MPa, 1.72 MPa, and 0.45 MPa at ε =5%, and those of the 5:1, 10:1 and 20:1 pure PDMS were 0.88 MPa, 1.10 MPa and 0.24 MPa, respectively.

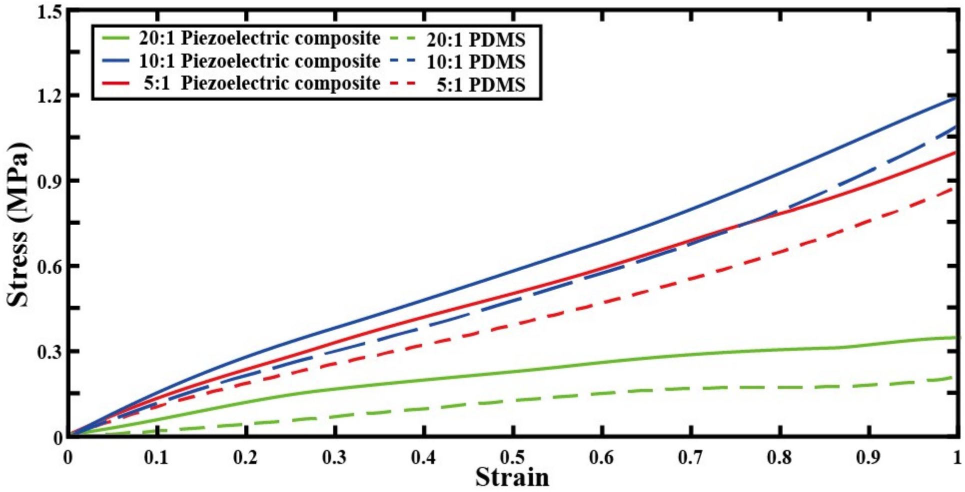

Figure S3. Stress-strain curves of the p-NCs and pure PMDS with different matrix mixing ratios.

4. Quasi-static cyclic tensile testing at 5%, 10% and 20% strain

Quasi-static cyclic tensile testings were conducted by MTS Insight 5 electromechanical test system. The hysteretic loops of 5%, 10% and 20% strain at a strain rate of 0.0025 s^{-1} are shown in Figure S4. The mixing ratios (λ) between PDMS monomer and curing agent were 5:1, 10:1 and 20:1, respectively.

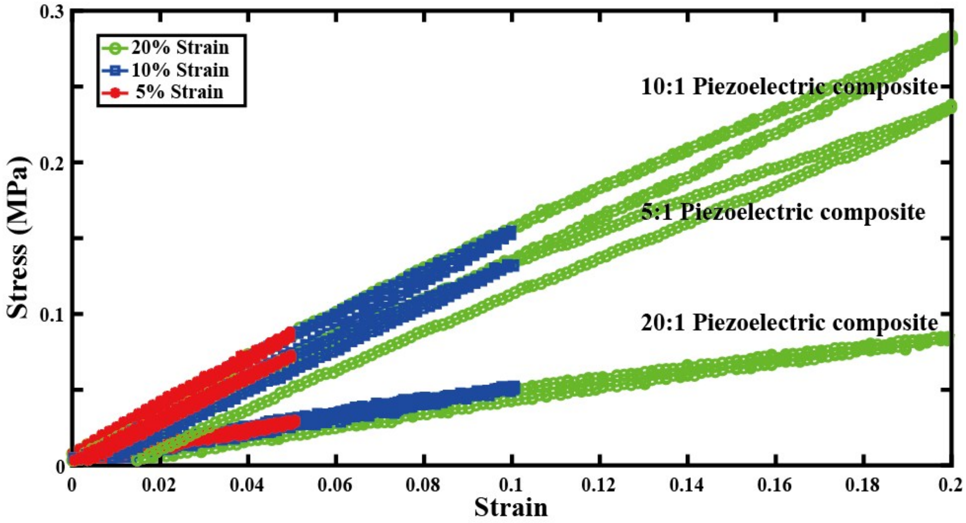

Figure S4. Cyclic tensile loading-unloading hysteretic loops of the p-NCs at different $strains\ (\varepsilon = 5\%, 10\%\ and\ 20\%)$.

5. Electrical poling

To align dipoles of synthesized p-NC, the poling process was conducted as follows.

1) Bring a sample with an electrode bonded into the “negative” side;

2) Place the sample as shown in the Figure S5 (a) below;

3) Connect the electrode into the stage/ground;

4) Place the upper compartment of the system to close the system;

5) The piezoelectric material (BTO NPs) needed be heated above Curie temperature (~ 130 °C) to have centrosymmetry followed by application of a strong electric field that aligns dipoles along the direction of the electric field. And, there is some heat loss when the heat was transferred from the PDMS matrix to BTO NPs. Therefore, we turn on the heating system to heat the stage up 140 °C which is slightly higher than the Curie temperature of BTO NPs. Keep monitoring the temperature throughout the poling process;

6) Once reached the desired temperature, turn on the high voltage power source (CZE1000R adjustable high voltage DC power supply, Spellman) to reach the electric field of 100 kV/cm;

7) Maintain the high voltage and temperature for 30 minutes;

8) Turn off the heating and let the set-up cool down with high voltage on until thermocouple reads ambient temperature;

9) Turn off the high voltage once reached ambient temperature;

10) Disconnect electrode and remove the sample.

(a)

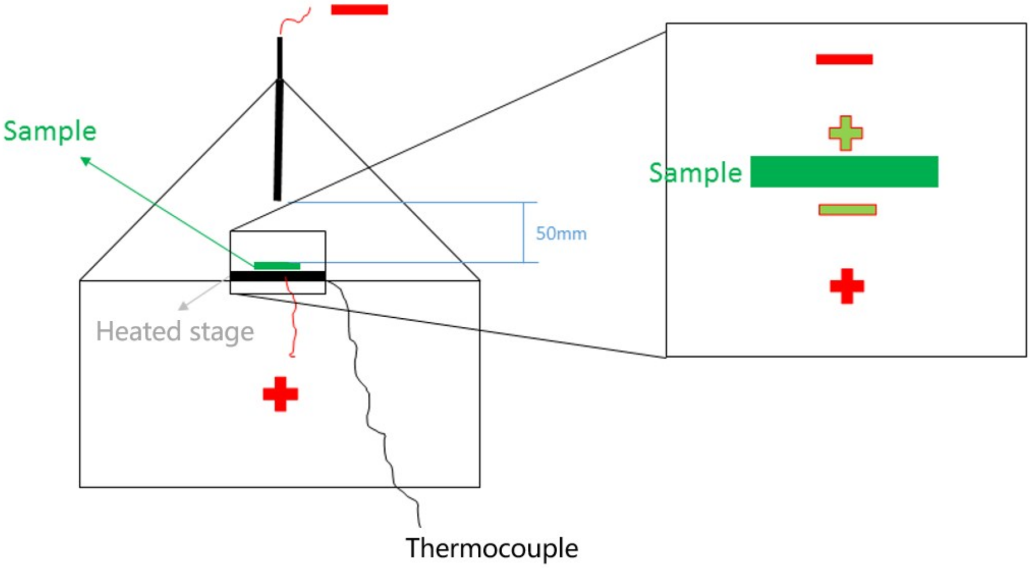

(b)

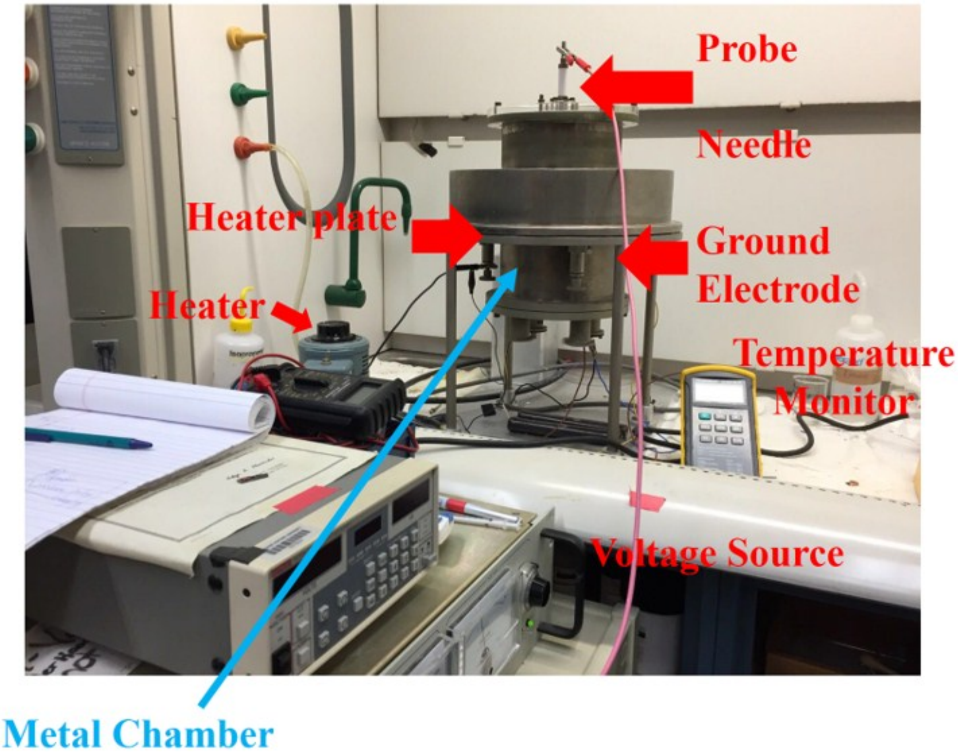

Figure S5. (a) Schematics of the electrical poling set-up and (b) the actual image.

6. Piezoelectric performance measurement set-up under quasi-static loading condition

For determining the piezoelectricity coefficient (d_{33}), Au/Cr electrodes were deposited on top and bottom surfaces of the p-NCs by sputtering. For the loading set-up, the bottom side plate was fixed to the frame and the loading force was applied by directly putting different weights on the top plate. The generated charges were measured by an electrometer (616 digital Electrometer, Keithley) and an oscilloscope (TDS2024B, Tektronix).

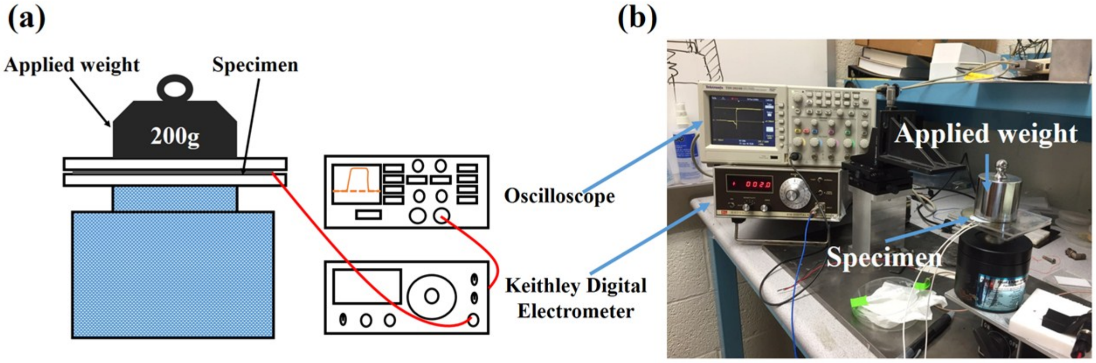

Figure S6. (a) Schematic of the quasi-static piezoelectric performance measurement set-up and (b) the photo of the actual set-up.

7. Calculated stored energy density and dissipated energy density under dynamic loading conditions

Based on the equation (10) and (11) in the main text, stored energy density and dissipated energy density were calculated as a function of loading frequency by normalizing to 1 MPa loading stress as shown in Figure S7.

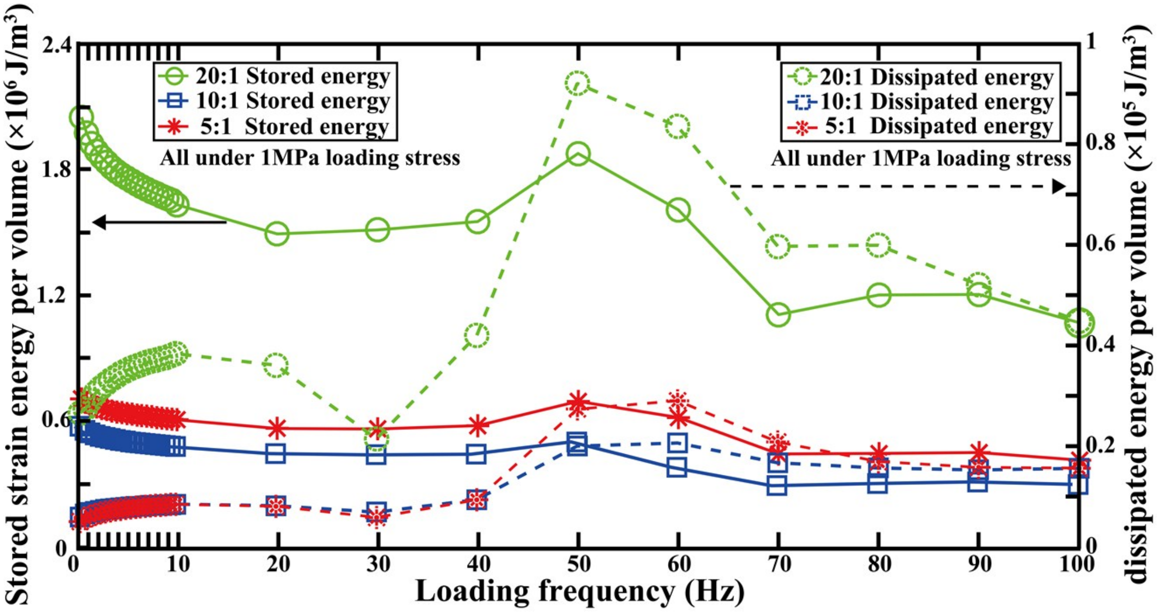

Figure S7. Calculated stored strain energy density and dissipated energy density as a function of a loading frequency.

8. Dielectric constant measurement

To decouple the influences of the loading frequencies on the electrical properties of the p-NCs, we measured the dielectric constants as a function of loading frequency. The p-NC was sandwiched between two insulated plates. One plate was attached to the mini-shaker while the other one was connected to the loading cell fixed to the support frame (Figure S8 (a)&(b)). The shaker was driven by a synthesized function generator (DS345, Stanford Research) and a piezo amplifier (EPA104, Piezo Systems). The loading stress was measured by a load cell (LRM200, 10 lb, Futek). The capacitance values of the p-NC during the dynamic compression stress were measured by the LCR meter (LCR-819, Instek).

As shown in Figure S8 (c), the dielectric constants of the p-NCs kept constant in the 1-100 Hz loading frequency range. The values of the dielectric constants were consistent with quasi-static condition. The permittivity of the 20:1, 10:1 and 5:1 p-NCs were ~3.95×10^{-11} F/m, ~3.26×10^{-11} F/m and ~3.04×10^{-11} F/m, respectively. The 20:1 p-NC with the largest portion of PDMS monomer showed the largest dielectric constant while the 5:1 p-NC showed the smallest one. The 20:1, 10:1 and 5:1 pure PDMS show the same trend with the dielectric constant of ~2.17, ~2.52 and ~2.93, respectively.

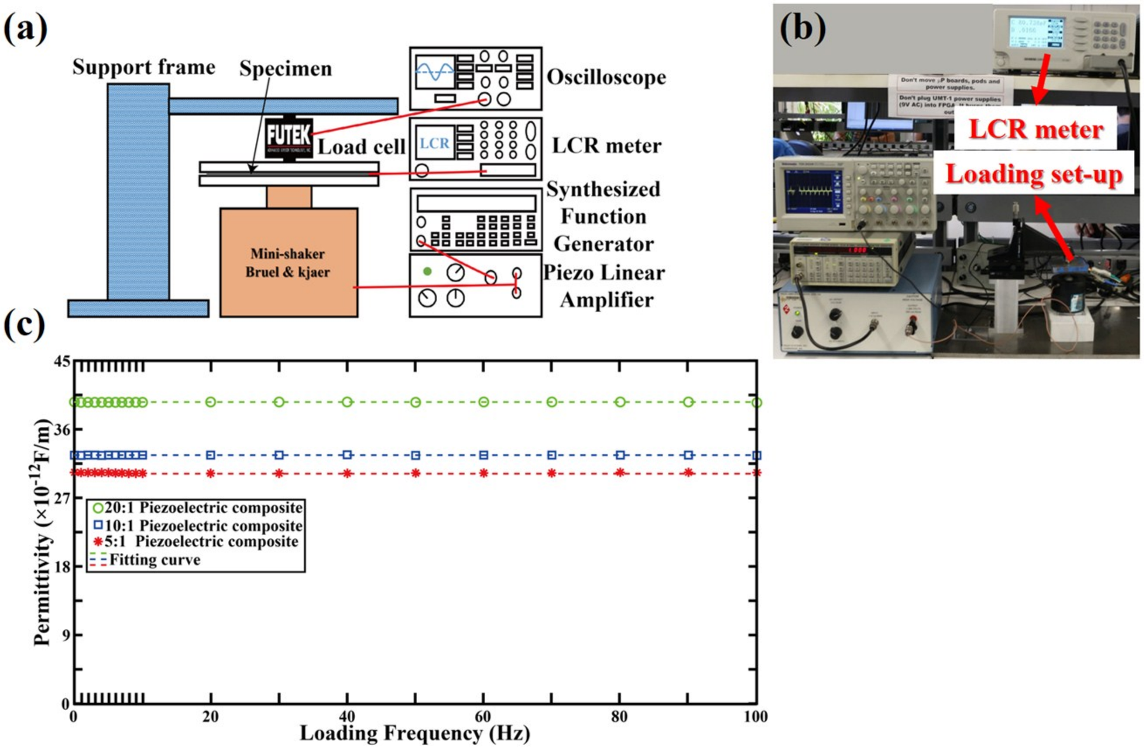

Figure S8. (a) Schematic of the dielectric constant measurement set-up under dynamic loading and (b) the photo of the actual measurement set-up. (c) The permittivity of the p-NCs as a function of loading frequency.

9. Piezoelectric performance measurement set-up under dynamic loading conditions and discussion of the output signals in a low frequency regime

Measurement set-up

For measuring the dynamic piezoelectricity coefficient (d_{33}'), p-NCs with Au/Cr electrodes were sandwiched between two insulated plates. One plate was attached to the mini-shaker while the other one connected to the load cell fixed to the support frame. The shaker was driven by a synthesized function generator (DS345, Stanford Research) and a piezo amplifier (EPA104, Piezo Systems). The loading stress was measured by the load cell (LRM200, 10 lb, Futek). The charge generated during the dynamic compression stress was measured by a charge amplifier (piezo film lab amplifier, TE Connectivity) and an oscilloscope (TDS2024B, Tektronix).

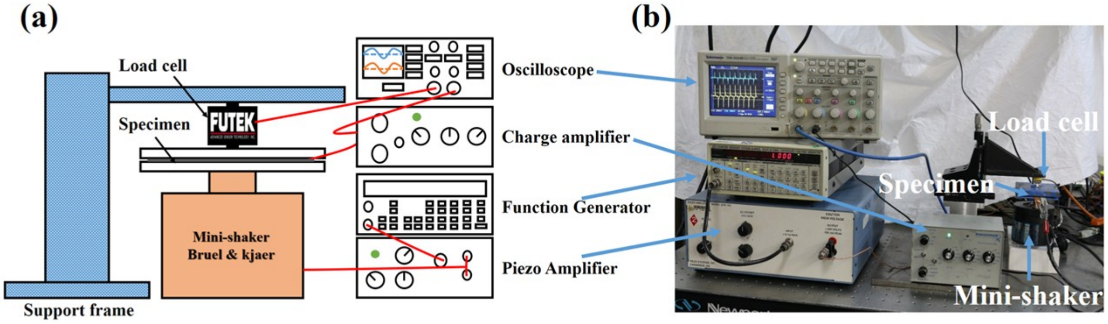

Figure S9. (a) Schematic of the dynamic piezoelectric performance measurement set-up and (b) the photo of the measurement set-up.

Discussion of output signals in a low frequency regime

To be noted here is due to instrumental limitation, one single loading pulse cannot last longer than 0.1s. This means, at low loading frequency (1-10 Hz), a single loading pulse cannot occupy one cycle time, while the system is at rest between loading pulses. However, with loading frequency increases (>10 Hz), each single loading pulse could fully occupy its own period. So, the gaps were eliminated. As a result, the loading pattern is transiting from repeating single pulses (quasi-static) to continuous sine wave (dynamic) as Figure S10(a). Thus, for comparison, we plotted estimations from quasi-static models versus the experimental results at 1-10 Hz (Figure S10(b)) as well. It clearly shows that the quasi-static model works better in a lower frequency regime, while the dynamic model is better when approaching 10 Hz.

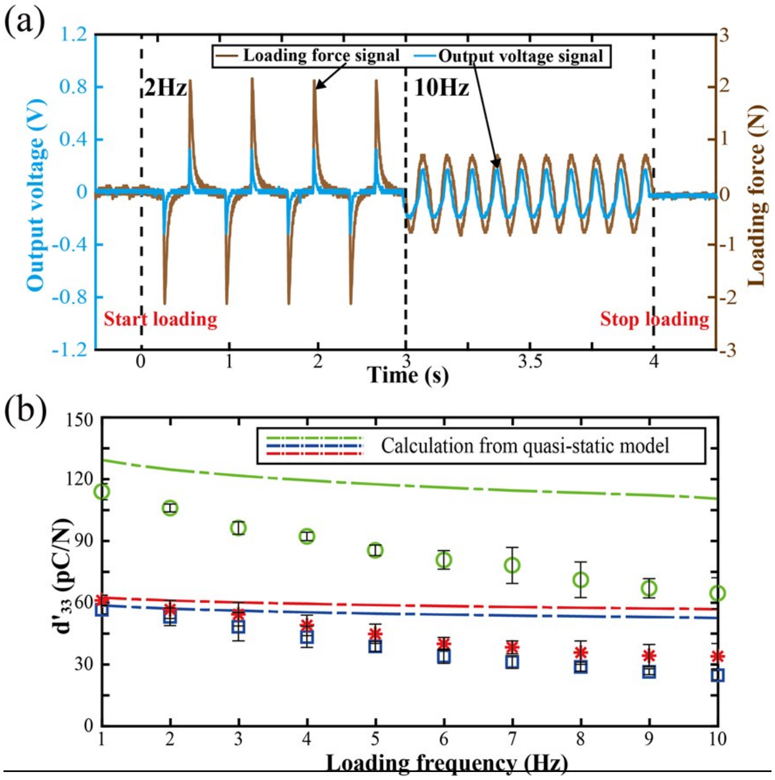

Figure S10. a) The repeated cycles of in-phase loading force signal and output voltage signal of 20:1 p-NC at 2 Hz (left) and 10 Hz (right). Both the applied force and voltage are plotted. b) The plots of estimations from quasi-static models vs. the experiment results at 1-10 Hz.

10. Charging a commercial capacitor using fabricated flexible 3D piezo-shells made of 20:1 p-NC, 10:1 p-NC and 5:1 p-NCs

Fabrication processes of the piezoelectric 3D shell structure

To verify the capability of the established numerical model for piezoelectric-viscoelastic systems in complex loading conditions, we fabricated 3D shell p-NCs with varied viscoelastic properties. The schematic of the assembly of the 3D shell fabrication mold is described as Figure S11 (a). The mold consists of a glass-filled PTFE rod (purchased from McMaster-Carr) with diameter of 16 mm and a glass-filled PTFE tube (purchased from McMaster-Carr) with inside diameter of 19 mm. After applying a lubricating grease (super lube silicone lubricating grease, Grainger Industrial Supply) to the surfaces of the rod and tube, the rod is fixed in the center of the tube by layered pedestal with grooves (Figure S11 (b)). Then, uncured p-NCs were injected to the gap between the rod and tube by using a syringe. The filled mold was put in the vacuum chamber to degas for 2 hours. Then, the p-NC was cured at 120 °C in the oven for 20 minutes, followed by 48 hours at room temperature. Finally, the 3D shell p-NC was obtained by removing the cured p-NC from the tube and rod. The 3D shell p-NCs with the Au/Cr electrode and conductive wires are shown in Figure S11(c).

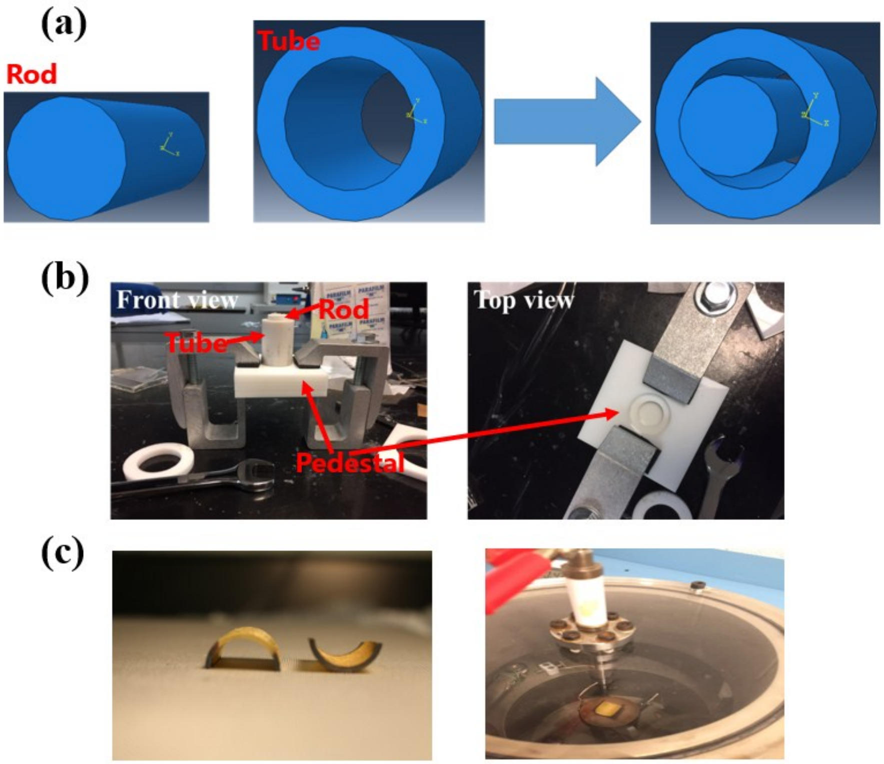

Figure S11. (a) Schematic of the fabrication of the mold for the 3D shell structures and (b) the actual image of the mold and the pedestal fixture. (c) The left image is the 3D shell p-NCs with Au/Cr electrode. The right image is the 3D shell p-NC under poling process.

Capacitor charging processes

As the equivalent circuit in Figure S12 (a) shows, the piezo-shell was sandwiched by two flat loading plates and connected to a predesigned rectifying circuit composed of a polarized capacitor and a bridge rectifier. Then, it was activated by 0.5 N compressing loading at 10 Hz to conduct the capacitor charging process. Figure S12 (b) shows the actual loading image. The generated alternating current (AC) piezoelectric output was fully rectified through the bridge circuit and simultaneously stored in a commercial 1000 pF capacitor available from SparkFun Electronics®. The entire charging process was recorded by monitoring the converted direct-current (DC) voltage/potential across the capacitor by using a Fluke 189 True RMS Multimeter. Figure S12 (c) shows the entire charging set-up image during the charging process.

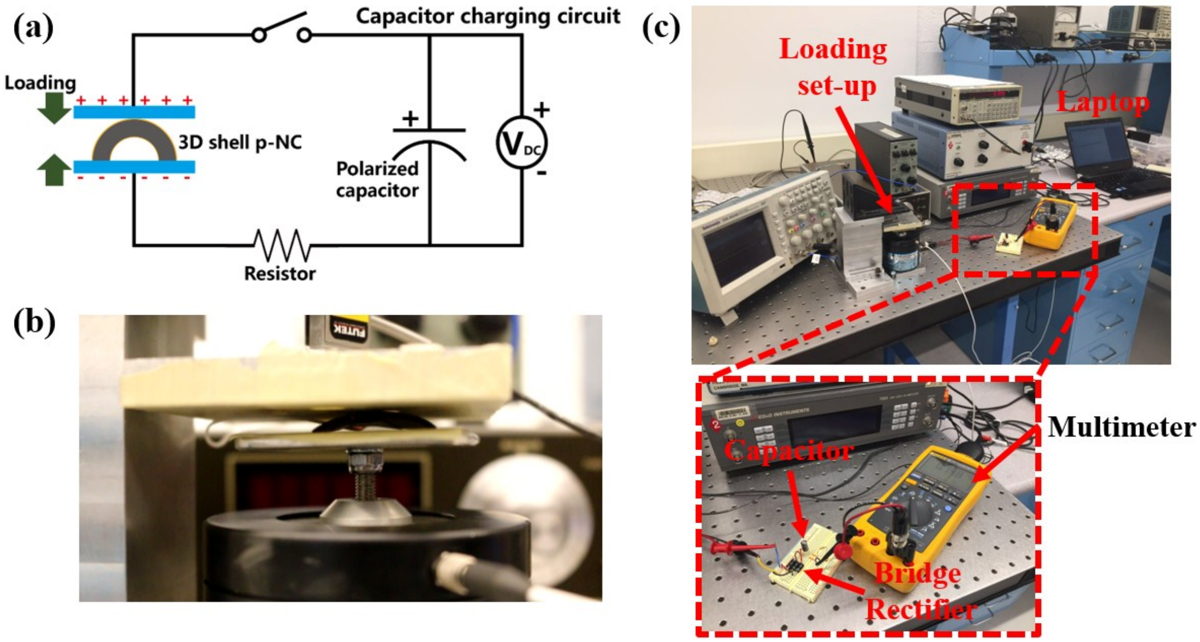

Figure S12. (a) Schematic of the equivalent charging circuit. (b) The actual loading image and (c) the image of entire charging set-up during charging process.